Article

Journal of
Biomedical Nanotechnology
Vol. 13, 1735–1746, 2017
www.aspbs.com/jbn

Efficacy of Different Compositions of Cerium Oxide Nanoparticles in Tumor-Stroma Interaction

Maren Sack-Zschauer[1,*], Elif Karaman-Aplak[1], Claudia Wyrich[1], Soumen Das[2], Thies Schubert[1], Hajo Meyer[3], Christoph Janiak[3], Sudipta Seal[2], Wilhelm Stahl[1], and Peter Brenneisen[1]

[1] *Institute of Biochemistry and Molecular Biology I, Medical Faculty, Heinrich-Heine University, Düsseldorf 40225, Germany*
[2] *Advanced Materials Processing and Analysis Center, Nanoscience and Technology Center (NSTC), Mechanical, Materials, and Aerospace Engineering (MMAE), University of Central Florida, Orlando, United States*
[3] *Institut für Anorganische Chemie und Strukturchemie, Heinrich-Heine Universität, Universitätsstr. 1, 40225 Düsseldorf, Germany*

The biomedical application of cerium oxide nanoparticles (nanoceria) is a focal point of research for a few years. The biochemical effects of nanoceria depend on various factors including particle size, oxidation state of cerium, oxygen vacancies on the surface, use of dispersants or coatings, pH and cell type. Due to their autocatalytic redox-activity, these particles are considered to act as a specific anti-cancer tool with less side effects on healthy cells and tissues, as the particles kill tumor cells, while protecting healthy cells from oxidative damage. In the present study, four different types of nanoceria were investigated with regard to their impact on biochemical parameters *in vitro*, which play a pivotal role in tumor-stroma interaction. The obtained data and presented *in vitro* test parameters will be helpful in designing nanoceria compositions, which are ideally suited for anticancer therapy, either as a 'stand alone drug' or in combination with other chemotherapeutics.

KEYWORDS: *Cerium Oxide Nanoparticles, Nanomedicine, Cancer, Melanoma, Tumor-Stroma-Interaction, Cancer Therapy.*

BACKGROUND

Numerous data dealing with neoplastic transformation and tumor progression solely focus on tumor cells and often address the question of how anticancer drugs affect tumor cell survival.[1–6] However, tumor cells interact with apparently normal (healthy) cells in their direct environment, called the tumor microenvironment. Here, a bilateral communication exists between cancer cells and the stroma,[7–10] which was initially thought to have only supportive function in tumor development. Yet, there is increasing evidence that stromal components actively take part in tumor progression, in immunosuppression, and in the development of drug resistance.[11–14] Beside immune cells, endothelial cells, soluble factors, and components of the extracellular matrix, another crucial cell type of the stroma is the cancer-associated fibroblast,[15,16] a modulated fibroblast expressing the biomarker alpha-smooth muscle actin (aSMA) and interacting with cancer cells in tumor invasion and angiogenesis.[13,15,17,18] Traditional options in the treatment of cancer comprise surgery, radiation therapy and/or chemotherapy, but often resulting in harmful side effects on healthy cells and holding the risk of late secondary cancer. Still, anthracyclines (e.g., daunorubicin, doxorubicin, epirubicin, idarubicin) are among the most effective antineoplastic agents, which are used for the treatment of many neoplastic diseases, both in non-solid and solid tumors, such as leukemia, Hodgkin's disease, non-Hodgkin's lymphoma, Wilms' tumor, lung, ovary, breast, prostate, and skin cancer.[19–21] Even though anthracyclines are frequently used, the incidence of severe side effects such as alopecia, vomiting, nausea, mucositis and cardiotoxicity, as well as the occurrence of drug resistance is well known.[21] In conclusion, the clinical application of such chemotherapeutics is limited in many cases.[3,22,23] In recent years, considerable efforts have been made to improve the therapeutic outcome of cancer chemotherapy and, finally, the quality of life of patients. In that context, monoclonal antibodies,[5,24] kinase inhibitors,[6] and proteasomal inhibitors[4] for anticancer therapy were developed

*Author to whom correspondence should be addressed.
Email: maren.sack@uni-duesseldorf.de
Received: 16 February 2017
Accepted: 23 September 2017

and already tested in clinical trials, often with only modest results. A rather novel field to improve anticancer therapies and to lower side effects is nanomedicine, the medical application of nanoparticles, whose size is 100 nm or below and, therefore, giving them exceptional therapeutical options.[25,26] One of the most important options of nanotechnology comprise drug delivery, i.e., transport of chemotherapeutics in nanoparticles to specific targets. For instance, the anticancer drug Doxorubicin was delivered to mitochondria of HeLa tumor cells with triphenylphosphonium functionalized mesoporous silica nanoparticles resulting in enhanced cell killing.[27] Furthermore, so-called nanopharmaceuticals, nanoparticles themselves acting as pharmacological substance, have recently been introduced as 'stand alone drugs'[28–30] or in combination with classical chemotherapeutical agents such as imatinib[31] or doxorubicin.[32,33] As the number of publications on the health effect of nanomaterials continuously increased over the last years, the attention for potential harmful effects is now a focal point[34] and, indeed, several *in vitro* and *in vivo* studies, especially with silver, zinc oxide, and titanium dioxide nanoparticles, have demonstrated adverse effects.[35–39]

On the other hand, cerium oxide (CeO_2/Ce_2O_3) nanoparticles (CNP, nanoceria) with oxidation states IV and III seem to have more beneficial effects due to their oxygen vacancies dependent characteristics.[40,41] These vacancy-engineered particles indicate antioxidative enzyme-mimetic activity, detoxifying hydroxyl radicals, superoxide, hydrogen peroxide, and peroxynitrite ($ONOO^-$) in cell-free test systems and in different cells and tissues *in vitro* and *in vivo*.[41–48] However, the outcome of some studies suggest that cerium oxide nanoparticles also trigger damaging mechanisms.[49,50] In our studies we recently showed a bifunctional role of dextran-coated and oxygen vacancies containing CNP, a prooxidative increase in cell killing and lowering of the invasive capacity of squamous skin carcinoma and melanoma cells while showing an antioxidative, rather protecting effect on (stromal) fibroblasts.[30,51,52]

The mode of action and cytotoxicity of nanoparticles even of the same type are often controversially discussed. Inconsistent data situation may depend, for example, on surface charge, size, zeta potential, coating, and biocompatibility of the nanoparticles as well as the surrounding environment, e.g., pH values.[42,53–56] In this study, four different types of nanoceria were investigated with regard to their efficacy on cell biological and biochemical parameters *in vitro*, which play a pivotal role in tumor-stroma interaction. These data can be a piece of the puzzle, which, in the future, should result in a cerium oxide nanoparticle composition ideally suited for an anticancer therapy, either as 'stand alone drug' or in combination with other chemotherapeutics.

MATERIAL AND METHODS

Chemicals, including cell culture medium Dulbecco's modified Eagle medium (DMEM), were obtained from Sigma or Merck Biosciences, unless otherwise stated. The fetal calf serum (FCS) was purchased from Pan Biotech. The Protein Assay Kit (Bio-Rad DC, detergent compatible) was from Bio-Rad Laboratories. The enhanced chemiluminescence system (SuperSignal West Pico/Femto Maximum Sensitivity Substrate) was supplied by Pierce. Penicillin/Streptomycin was obtained from Biochrom and Glutamax from Gibco. The monoclonal mouse antibodies raised against human α-tubulin and α-smooth muscle actin (αSMA) were obtained from Sigma. The polyclonal horseradish peroxidase (HRP)—conjugated rabbit anti-mouse IgG antibody (DAKO) was used as secondary antibody.

Cell Culture

The human malignant melanoma cell line A375, originally derived from a 54-year-old woman, was purchased from ATCC (ATCC®CRL-1619™).[57] Human dermal fibroblasts (HDF) were purchased from Promocell (NHDF f-c.) and were originally isolated from the dermis of juvenile foreskin of a healthy donor. HDF were used in passages 2 to 12, corresponding to cumulative population-doubling levels of 3 to 27.[58] Human melanoma cells and HDFs were cultured in low glucose DMEM (Sigma) supplemented with 10% FCS (FBS Premium, Pan Biotech). For treatment with CNP cells were cultured in serum free high glucose DMEM (Sigma).

Cerium Oxide Nanoparticles

CNP-2 (Ce IV, water based suspension; 1.5 mg/ml, 1–10 nm) were purchased from Scivention and are stabilized in sodium polyacrylate (1.27 mg/ml). CNP-3 (Ce IV, water based suspension, 10 wt.%, <25 nm) were purchased by Sigma. CNP-4 (JRCNM02101a) were obtained from European Commission, Joint research center, Directorate I, Institute for Health and Consumer Protection in form of powder. It was dissolved (8.7 mM) in water by stirring and sonication for 1 hour. CNP-1 (Ce III/Ce IV, 5 mM, dextran coated, 3–5 nm) were synthesized in dextran (molecular weight: 1,000 Da) using previously described methods.[59] Briefly, stoichiometric amounts of dextran were dissolved in deionized water followed by cerium nitrate hexahydrate. The solution was stirred for 2 hours followed by addition of ammonium hydroxide (30%, w/w). The pH of the solution was kept below 9.5 to avoid precipitation of cerium hydroxide.

Dynamic Light Scattering (DLS) Measurements

DLS determines the size of particles (typically in the sub micron region) by measuring their Brownian motion with

light scattering. The Brownian motion is the random movement of particles suspended in a solvent caused by collisions with molecules in the surrounding medium. The velocity of the Brownian motion is defined by a property known as the translational diffusion coefficient, which is used by the calculation of the size of particles with the Stokes-Einstein equation;

$$d(H) = \frac{kT}{3\pi\eta D}$$

where $d(H)$ is the hydrodynamic diameter, D is the translational diffusion coefficient, k is the Boltzmann's constant, T is the absolute temperature, η is the viscosity.

All DLS measurements were carried out using a Zetasizer Nano S (Malvern Instruments Ltd., U.K.). The Nano S uses a 4 mW He–Ne laser operating at a wavelength of 633 nm and a detection angle of 173° (backscattering detection). The size and size distribution of all cerium oxide nanoparticles were determined in a solution with a minimum concentration of 0.5 mg/ml. Each sample was measured three times at a constant temperature of 20 °C. The instrument software was used to calculate the volume-weighted size distributions and to create the graphs.

UV/VIS Spectrometry

For UV/VIS spectrometric analyses the transmission of a 1 mM CNP solution in phosphate buffered saline (PBS) was used. PBS was used as a blank. The transmission of the solutions was measured with an Ultospec3000 photometer (Pharmacia Biotech) in a range between 190 and 1100 nm. The 1 mM CNP solution was oxidized with 75 mM H_2O_2 and the spectra were recorded again.

Cell Viability

The cell viability was measured by 3-(4,5-Dimethylthiazol-2-yl)-2,5-diphenyltetrazolium bromide (MTT) assay.[60] The reduction of MTT (Sigma) by mitochondrial dehydrogenases to formazan indicates the metabolic activity of cells and is an indicator of cellular viability. Briefly, serum-free medium containing MTT (0.5 mg/mL) was added to the cells after incubation with different concentrations of CNP. After incubation with MTT, cells were washed with PBS and lysed in DMSO. The formation of the blue formazan was measured at 570 nm. The results were presented as percentage of untreated controls, which were set at 100%.

Preparation of Conditioned Media (CM)

The CM was obtained from HDFs (CM_{HDF}) and myofibroblasts (CM_{MF}). For this, seeded 1.5 Mio HDFs were grown to subconfluence (70% confluence) in 10 cm diameter dishes. The serum-containing medium was removed, and after washing in PBS, the cells were treated with 10 ng/ml or without rTGFβ1 in a serum-free DMEM for 48 h. This medium was removed, and after washing in PBS, all cells were incubated in 5 ml serum-free DMEM for further 48 h before collection of the CM_{HDF} and CM_{MF}. The CM was freshly used or stored at −20 °C up to 2 weeks before use.

Invasion Assay

Cell culture inserts (transwells) were covered with 125 mg/ml growth factor-reduced Matrigel and placed in a 24-well plate. A375 melanoma cells (5×10^4 cells/insert), either mock-treated or pretreated with 150 μM CNP (representing 25,8 μg/ml), were seeded on top of the Matrigel in a serum-free DMEM. CM_{HDF} and CM_{MF} were used as chemoattractants in the lower chamber. After 48 h at 37 °C, the melanoma cells were removed of the upper side of the filter using cotton swabs and the A375 cells, which invaded toward the lower side of the insert, were stained with Coomassie Blue solution (0.05% Coomassie Blue, 20% MeOH, and 7.5% acetic acid). The number of invaded cells was counted.

Measurement of Reactive Oxygen Species (ROS)

The intracellular ROS level was measured using the fluorescent dye H_2DCF-DA, which is cell membrane permeable and is intracellular hydrolyzed to the non-fluorescent derivative H_2DCF. In the presence of peroxides, H_2DCF is converted into the fluorescent DCF (2′,7′-dichlorofluorescein). For assays, subconfluent A375 melanoma and HDF monolayer cultures were loaded with 100 μM H_2DCF-DA in Hank's balanced solution buffer (HBSS, Sigma) for 30 min at 37 °C. After washing with HBSS, the loaded cells were subjected to 300 μM CNP in HBSS. ROS generation was detected as a result of the oxidation of H_2DCF and the fluorescence intensities (excitation 480 nm; emission 520 nm), given in relative fluorescence units, were measured with Optima Fluostar platereader (BMG labtech) for 90 min in 5 min intervals.

SDS-PAGE and Western Blotting

Sodium dodecyl sulfate-polyacrylamide gel electrophorese (SDS-PAGE) was performed according to the standard protocols published elsewhere[61] with minor modifications. Briefly, cells were lysed after incubation with CNP 1–4 in 1% SDS with 1:1000 protease inhibitor cocktail (Sigma). After sonication, the protein concentration was determined by using a modified Lowry method (Bio-Rad DC). SDS-PAGE sample buffer (1.5 M Tris-HCl pH 6.8, 6 mL 20% SDS, 30 mL glycerol, 15 mL β-mercaptoethanol, and 1.8 mg bromophenol blue) was added, and after heating, the samples (20–30 μg total protein/lane) were applied to 10% (w/v) SDS-polyacrylamide gels. After blotting, immunodetection was carried out (1:1000 dilution of primary antibody (anti-αSMA, Cell Signaling; 1:20000 dilution of anti-mouse antibody conjugated to HRP). Antigen–antibody complexes were visualized by an

enhanced chemiluminescence system (Pierce). α-tubulin or Coomassie staining was used as internal control for equal loading.

Long Term Experiment

To examine the effects of a long term exposure to CNP in subconfluent A375 melanoma cells and HDF were incubated with 150 or 300 μM CNP-2 in serum free DMEM-high glucose (4500 mg glucose/l). After 96 h cells were trypsinized and the cumulative population doubling (CPD) was calculated by cell counting. For regeneration cells were cultured in DMEM—low glucose (1000 mg glucose/l) supplemented with 10% FBS for 72 h. Thereafter, the 96 h treatment followed by trypsinizing and culturing in 10% FBS DMEM was repeated finally 19 times.

RESULTS

Size Distribution of CNP

Dynamic light scattering (DLS) is a widely used technique to determine the size and the size distribution profile of nanoparticles in solution.[62] Figure 1 shows the size distribution of all cerium oxide nanoparticles (CNP 1–4), whereas the average sizes (calculated with the software of Zetasizer) are presented in Table I. CNP-1 and CNP-2 have the smallest diameter with an average size of 4.5 ± 1.7 nm (±standard deviation) and 4.7 ± 3.6 nm. In contrast to CNP-1 and CNP-2 the nanoparticles CNP-3 and CNP-4 show an increase in size and a broader diameter distribution. CNP-3 have an average size of 76.4 ± 29.7 nm, whereas CNP-4 show two peaks at 188.6 ± 128.4 nm and 5046 (±855,3) nm, which may be due to agglomeration of the particles.

Redox-Activity of CNP

The redox-activity of CNP and in consequence the biological activity is described to be dependent of the content of Ce^{3+} and Ce^{4+} as well as on oxygen vacancies on the surface of the particles.[63] UV-visible transmission spectra of the nanoparticle solution provide indications for the

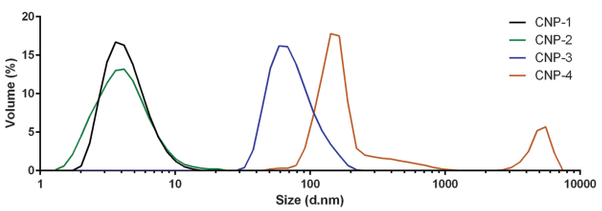

Figure 1. Particle size distribution of cerium oxide nanoparticles. Dynamic light scattering (DLS) measurements were carried out to determine the size distribution of CNP-1 (A), CNP-2 (B), CNP-3 (C) and CNP-4 (D). The graphs represent the average results of three independent measurements (created by the software of Zetasizer), which show the volume-based size distribution as diameter (in nm). All measurements were performed three times.

Table I. The average particle size of cerium oxide nanoparticles (CNP) measured by DLS and calculated by the software of Zetasizer.

CNP	*D* (nm)[a]
1	4,5 (±1,7)
2	4,7 (±3,6)
3	76,4 (±29,7)
4	188,6 (±128,4)
	5046 (±855,3)

Notes: [a]*D* (nm): Average particle size as diameter, reported as mean ± standard deviation.

Ce^{3+}/Ce^{4+} ratios. In the presence of Ce^{3+} on the particles surface, a red-shift (a shift of UV absorption spectra into longer wavelengths) can be observed after the oxidation with H_2O_2. This shift is postulated to be caused by a change in the oxidation state from Ce^{3+} to Ce^{4+}.[64–67] The UV-visible transmission spectra of all nanoparticle solutions (1 mM in PBS) were recorded before and after oxidation with H_2O_2 and are presented in Figure 2. The transmission spectra of CNP-1 and CNP-2 are comparable and both show the above mentioned red shift. After oxidation with H_2O_2 a shift to longer wavelength (=red shift, around 100 nm) was observed in CNP-1 and CNP-2 solutions. In contrast, CNP-3 and CNP-4 showed different transmission characteristics. CNP-3 absorbs UV/VIS light in broader range, but no shift after H_2O_2 treatment was detectable. CNP-4 only showed a marginal shift after oxidation with H_2O_2.

Cytotoxicity of CNP

The biological activity of CNP comprising cytotoxic effects are dependent on several factors including particle size, Ce^{3+}/Ce^{4+} ratio, use of dispersants, solution pH etc., and especially on cell type. For a potential use of CNP as chemotherapeutic agent it is crucial to determine the impact on viability of tumor cells and also on normal, healthy cells, as systemic application would act on all cells and tissues, not alone on tumor cells. The effects of the different cerium oxide nanoparticles on cell viability were assessed by performing MTT assays with A375 melanoma cells and human dermal fibroblasts (Fig. 3), as fibroblasts are the most common cells of the skin and play a pivotal role in tumor-stroma-interaction.[16] All of the tested CNP exerted cytotoxic effects in A375 melanoma cells, whereas CNP-1 and CNP-2 were the most toxic particles with IC_{50} values of around 150 μM and 250 μM. Moreover, at a concentration of 1500 μM CNP-1 and CNP-2 the cell viability was decreased to 38% and 28% compared to the untreated control. CNP-3 showed an IC_{50} of around 250 μM, as well, but at higher concentrations the cell viability was not further decreased in contrast to CNP-2, which showed a concentration dependent decrease. For CNP-4 no IC_{50} could be determined in A375 cells, as with the highest tested concentration (1500 μM) the cell

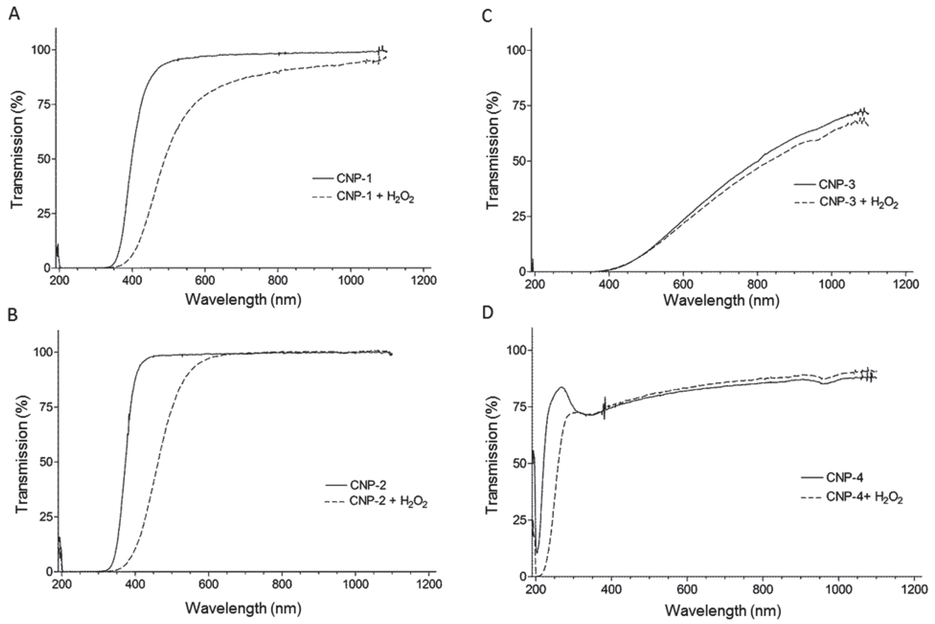

Figure 2. **Transmission characteristics and redox-activity of different CNP. UV/VIS transmission spectra of 1 mM CNP before and after oxidation with 75 mM H_2O_2. The shift towards higher wavelengths (red shift) is due to a change in the oxidation state from Ce^{3+} to Ce^{4+} indicating the content of Ce^{3+} within the particles and also demonstrating the redox-activities of the particles.**

viability was decreased to 57%. None of the tested particles showed cytotoxic effect in HDF with exception of CNP-3, which decreased the cell viability of HDF to 70% at a concentration $\geq$500 μM compared to the untreated controls.

Invasive Capacity of CNP on Melanoma Cells

The most critical step in progression of melanoma is the invasion of tumor cells. Therefore, we tested the effect of CNP on tumor cell invasion capacity using conditioned media of fibroblasts (CM_{HDF}) and myofibroblasts (CM_{MF}) as chemoattractant (Fig. 4). Conditioned medium of myofibroblasts contains proinvasive signals (e.g., Il-6, VEGF, HGF)[9] and thus serves as a positive control in this assay. After treatment for 48 hours all tested CNP decreased the number of invading tumor cells, whereas in CM_{MF} CNP-1 shows the highest anti-invasive impact with a decrease to 20% invaded tumor cells compared to the untreated control, followed by CNP-3 and CNP-4 (30 % and 32%). In CM_{HDF} the number of invading tumor cells was lowered as well, but to a lesser extent compared to tumor cells, which invaded towards CM_{MF}. CNP-2 showed less anti-invasive impact on the melanoma cells compared to the other tested particles, nonetheless diminished the number of invading tumor cells to 55% in CM_{MF} and 70% in CM_{HDF}.

Impact of CNP on Myofibroblast Formation

The TGF-β1 mediated transition of fibroblasts to myofibroblasts is ROS dependent[9] and plays a pivotal role in tumor invasion, as myofibroblasts form an invasive front

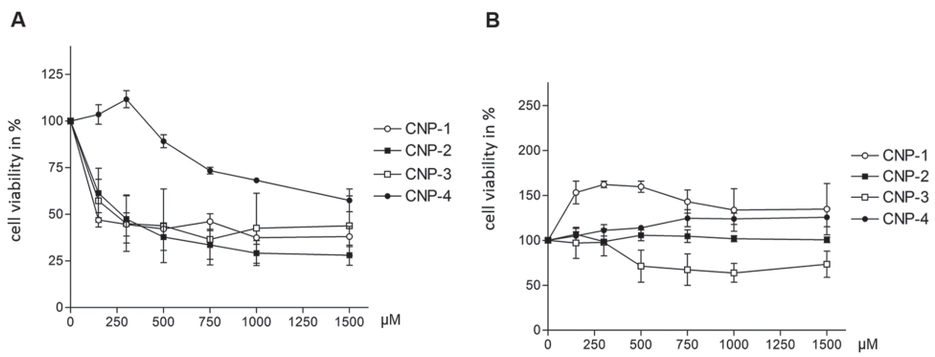

Figure 3. **Toxicity of CNP in tumor cells and healthy cells. Subconfluent A375 melanoma cells (A) and human dermal fibroblasts (HDF, B) were treated with different concentrations of CNP for 96 h. Cell viability was assessed by MTT assay. The percentage of cell viability in comparison to the untreated control, which was set to 100%, is presented. Data are presented as means ± SEM.**

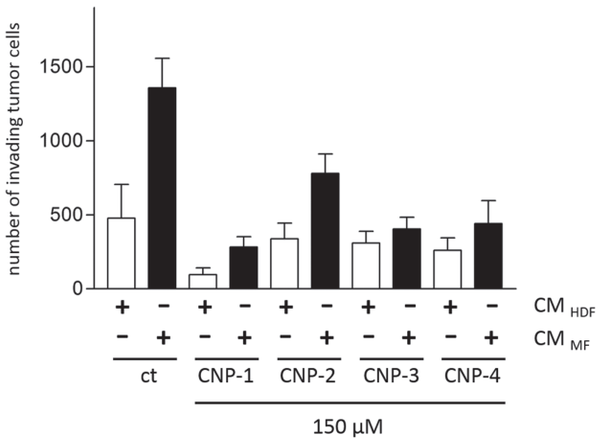

Figure 4. **Effects of different CNP on tumor cell invasion. Subconfluent melanoma cells (A375) were treated with 150 μM CNP or mock-treated for 48 h before used for invasion assays. The invasive capacity of these cells was tested with conditioned medium of HDFs (CM_{HDF}) and myofibroblasts (CM_{MF}), which was used as chemoattractant. The data represent the mean ± standard error of the mean (SEM) of three independent experiments. *$p < 0.05$ versus CM_{MF} (Student's *t*-test).**

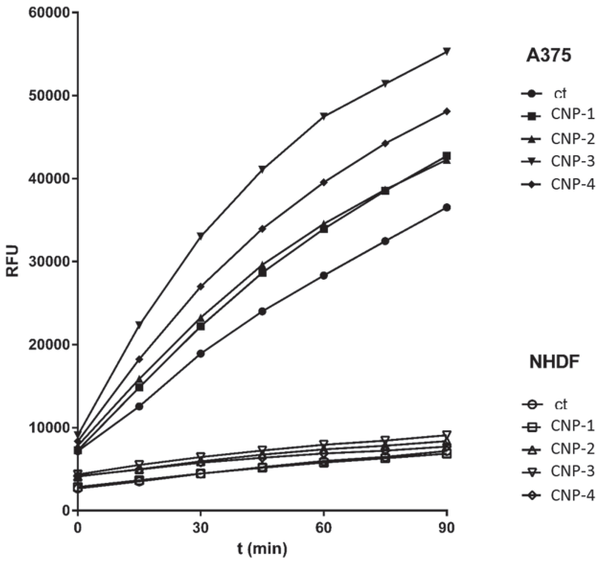

Figure 6. **Effect of different CNP on intracellular ROS levels. Subconfluent A375 melanoma cells and human dermal fibroblasts were incubated with H_2-DCF-DA for 30 min and excess DCF was removed. Afterwards cells were treated with 300 μM CNP and fluorescence intensities were measured for 90 min in 5 min intervals. A representive measurement of three independent experiments are presented.**

supporting the degradation of the extracellular matrix and thereby enhancing invasion of tumor cells.[16] Hence, we studied the effect of the various CNP on myofibroblast formation by determining protein levels of α-smooth muscle actin (αSMA), which is used as a marker for myofibroblasts (Fig. 5). Therefore, HDF were pretreated with the different types of CNP for 24 h or 48 h followed by a 48 h treatment with recombinant TGFβ-1 to induce myofibroblast formation. The αSMA levels in fibroblasts were decreased after 24 h and 48 h of treatment with each of the tested particles, however CNP-4 is the most effective showing a decrease to 24% after 24 h and to 14% after 48 h compared to the TGF-treated control. In comparison CNP-1, CNP-2 and CNP-3 lowered the αSMA levels in TGF-treated HDF to 58%, 77% and 66% after 24 h pretreatment, respectively.

Intracellular ROS Generation by CNPs

Numerous studies show that cerium oxide nanoparticles exhibit a redox-activity in cell free system, in different cell lines and also in animal models, though the results are still contradictory.[41, 45–47, 66, 68] Antioxidant, but also prooxidative effects of CNP were found depending on experimental settings, composition of the particles and environmental conditions that were mentioned

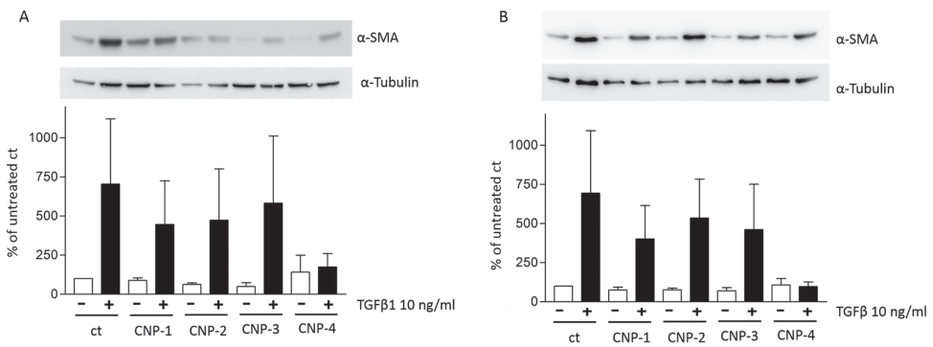

Figure 5. **Effect of CNP on TGFβ1-induced and ROS-mediated myofibroblast formation. Subconfluent HDF were incubated with 150 μM CNP for 24 h (A) or 48 h (B) before treatment with 10 ng/ml TGFβ1 (black columns) for further 48 h. After TGFβ1-treatment cells were lysed and prepared for western blot analyses to detect αSMA protein levels. A representative Western Blot and the x-fold change versus untreated controls of the densitometric analyses (mean intensities ± SEM) of three independent experiments is shown. α-tubulin and coomassie staining were used as loading controls.**

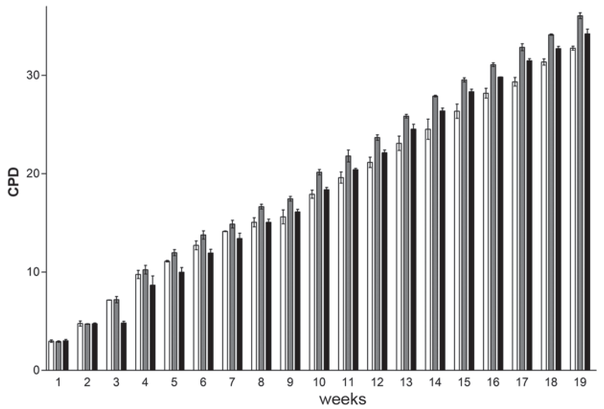

Figure 7. Influence of CNP long term exposure on proliferation of HDF. HDF were incubated with 150 μM (grey bars) or 300 μM (black bars) CNP-2. After 96 h cells were trypsinized and the cumulative population doubling (CPD) was calculated. For regeneration cells were cultured in DMEM—low glucose (1000 mg Glucose/l) supplemented with 10% FBS for 72 h. Thereafter, the 96 h treatment followed by trypsinizing and culturing in 10% FBS DMEM was repeated 19 times. Ct = white bars.

above. To measure the effect of the set of particles on ROS generation in A375 melanoma cells and human dermal fibroblasts the fluorescent dye DCF was used, which detects intracellular peroxides (Fig. 6). All of the studied CNP increased the ROS levels in tumor cells after 90 min treatment, while in HDF only a slight increase was detected. Most potent ROS generation in tumor cells was observed for CNP-3, which showed a 2.7-fold increase of the intracellular ROS level compared to the untreated control. Additionally, melanoma cells (untreated controls) were found to show 2.5-fold higher ROS levels compared to human dermal fibroblasts (untreated controls).

Influence of CNP on Proliferation After Long Term Exposure

Regarding a potential use as therapeutic tool, it is crucial to study the biological effects of a CNP long term exposure. We investigated the effect of a CNP long term exposure on proliferation of dermal fibroblasts to exclude adverse late effects. The cells were treated with 150 μM or 300 μM CNP for 96 h followed by a regeneration phase of 72 h in CNP-free medium. This treatment was repeated 18 times, so that the cells were exposed to CNP for a total of 19 weeks with 72 h of regeneration per week. Each week the cumulative population doubling (CPD) was determined by cell counting. A 300 μM (150 μM) CNP long term exposure did not affect the CPD of HDF (Fig. 7).

DISCUSSION

Previous studies showed that cerium oxide nanoparticles exhibit a great potential for future anti-cancer therapies. The particles selectively exert cytotoxic and prooxidative effects in several tumor cell lines *in vitro*[55,69–72] and also show an anti-cancer activity in *in vivo* xenograft mouse models.[30] Other studies revealed an antioxidant-mimetic protection in normal healthy cells and tissues from reactive oxygen species *in vitro* and *in vivo*.[44,45,73] However, different types of CNP were used in numerous studies leading to different, often contrary results, even if the studies deal with the same or similar scientific questions. Physical parameters of the particles such as size, structure, surface charge/oxidation state and others play an important role in that context. In conclusion, these data are often not comparable and reproducible, even though comparability and reproducibility of data are decisive for a therapeutic use of nanoparticles. In this study four different cerium oxide nanoparticles compositions (CNP-1–4) were tested on the basis of pivotal biological parameters in context of tumor-stroma interaction, like cytotoxicity, modulation of tumor invasion and ROS dependent myofibroblast formation. Moreover, proliferation after long term exposure in healthy cells (HDF) was studied. The herein tested CNP were obtained from diverse sources and differ in methods of synthesis method, size, coatings/dispersants, oxidation state (Ce^{3+}/Ce^{4+} contents), oxygen vacancies on the surface and agglomeration behavior (see Materials and Methods). In previous studies, CNP-1 were well characterized regarding physicochemical properties and biological activity.[53,59] Thus CNP-1 can be defined as reference or standard for this study. The results of the study are summarized in Table II for a brief overview.

CNP-1 and CNP-2, which were found to be the smallest of the tested particles with a diameter of around 4.5 nm, displayed the highest killing efficacy in tumor cells, while being nontoxic in human dermal fibroblast, which were used in our study as model for healthy stromal cells of the skin. Interestingly, both particles showed similar transmission spectra and red-shifts after oxidation with H_2O_2, indicating similar Ce^{3+}/Ce^{4+} ratios, and thus presumably comparable redox-activities. As previous studies showed that CNP-1 have a balanced ratio of Ce^{3+} and Ce^{4+} in aqueous, neutral dispersions,[52,66] it can be assumed from the comparison with the transmission spectra of CNP-1, that under these conditions CNP-2 may have a balanced ratio as well. CNP-3 and CNP-4, found to be larger in size in aqueous solution, were less toxic in tumor cells and showed different transmission characteristics compared to CNP-1 and CNP-2, with only a slight or no shift after oxidation with H_2O_2, implying different Ce^{3+}/Ce^{4+} ratios and redox-activities related to CNP-1/2. Based on the comparison to the spectrum of CNP-1, for which a balanced ratio in neutral pH is described,[52] it can be postulated that the ratios of CNP-3 and CNP-4 are not balanced. They seem to be shifted towards a higher Ce^{4+} content in the case of CNP-3 and towards Ce^{3+} in case of CNP-4. Additionally, both particle types do not react with H_2O_2 in the way CNP-1 or CNP-2 do, as there were no or only

Table II. Effects of different nanoceria compositions on tumor cells (A375) and healthy stromal cells. Arrows indicate an increase (↑) or a decrease (↓) of the investigated parameter. The number of arrows shows the extent of in- or decrease. N.d. = not detectable.

	CNP-1		CNP-2		CNP-3		CNP-4	
Size in aqueous solutions (DLS)	4.5 nm		4.7 nm		76.4 nm		188.6 nm	
Redox-activity (red shift in UV/VIS-spektra after reaction with H_2O_2)	Shift		Shift		No shift		Small shift	
Cell type	A375	HDF	A375	HDF	A375	HDF	A375	HDF
Cytotoxicity (MTT)	IC_{50}: 150 μM	(–)	IC_{50}: 250 μM	(–)	IC_{50}: 250 μM	Toxic $\leq$ 300 μM	n.d. IC_{50} (–l.5 mM)	(–)
Anti-invasive capacity (invasion assay)	↓↓↓	–	↓	–	↓↓	–	↓↓	–
ROS formation (after 90 min, DCF)	↑↑	↑	↑↑	↑	↑↑↑	↑↑	↑↑	↑
Myofibroblast formation (aSMA protein levels)	–	↓↓	–	↓	–	↓	–	↓↓↓

minor red shifts observed. The shift of CNP in aqueous solution to higher wavelength upon reaction with H_2O_2 is described to be the oxidation of Ce^{3+} to Ce^{4+}:[64,74]: Furthermore, these results suppose that a balanced ratio of Ce^{3+} and Ce $^{4+}$ is needed for a reaction with H_2O_2. In literature different and often contrary hypotheses can be found regarding the chemical reaction of CNP with H_2O_2. Some research groups postulate a catalase mimetic activity of CNP, whereupon H_2O_2 is detoxified into molecular oxygen and water.[47] Others describe a Fenton-like or a peroxidase-like reaction, where the highly reactive hydroxyl radical is produced.[66,75,76] The low toxicity of CNP-3 and CNP-4 on tumor cells may be based on an altered redox-activity, due to different Ce^{3+}/Ce^{4+} ratios compared to CNP-1 and CNP-2. In a study about the role of surface valence state effects, Pulido-Reyes et al. observed in i.a. that the toxicity of CNP depends on the Ce^{3+}/Ce^{4+} contents and consequently on the oxygen vacancies on the surface.[63] Additionally, the particle internalization strongly depends on the particle size.[77,78] Accordingly, another reason for the decline in killing efficacy of CNP-3 and CNP-4 in tumor cells could be a decreased uptake into the tumor cells, due to the enlarged size or enhanced particle agglomeration of CNP-3 and CNP-4 compared to the considerably smaller CNP-1 and CNP-2.

The invasion of tumor cells is a crucial event in tumor progression and metastasis. Besides killing of tumor cells, another aim of a therapeutic approach is the prevention of tumor cell invasion. CNP-1 showed anti-invasive effects in tumor cells, but also indirectly via blocking of myofibroblast formation.[30,52] Surprisingly, despite their different physicochemical properties regarding size and Ce^{3+}/Ce^{4+} ratios, all tested particles revealed anti-invasive effects in A375 melanoma cells, whereas the invasive capacity of melanoma cells was most efficiently decreased by CNP-1. Tumor cells often require the support of the surrounding stromal cells for their invasive performance.[16] As the TGFβ-1-induced and ROS-mediated formation of tumor-promoting myofibroblasts is a crucial factor in progression and invasion of malignant melanoma and squamous cell carcinoma,[9] the influence of the particles on the pro-invasive transition of fibroblasts to myofibroblasts was investigated. All particles showed inhibitory effects on myofibroblast formation, yet to different extents (see Table II), again showing anti-invasive activity of the tested particles. As CNP-4 showed the most drastic effect in this context, a smaller size or a balanced Ce^{3+}/Ce^{4+} ratio seem to be of no benefit regarding the prevention of myofibroblast formation. The results on the transition of fibroblasts may suggest an antioxidant activity of the particles in HDF, as myofibroblast formation is triggered by ROS. Nevertheless, ROS measurements did not confirm this suggestion, as an antioxidant effect was not detected after 90 min. In contrast, a slight increase of ROS was detected in CNP-treated HDF compared to the untreated controls. Remarkably, the ROS formation of tumor cells increased to higher levels after treatment with CNP compared to treated fibroblasts. Additionally, the A375 melanoma cells showed higher ROS levels compared to HDF under untreated conditions (2.5 fold). Increased ROS levels and in consequence an altered redox-status of the cell provide a specific vulnerability of cancer cells, which can be exploited in therapeutic approaches.[79,80] Usually, the imbalance between the prooxidative and antioxidative systems towards higher ROS levels in cancer cells is maintained under a cytotoxic threshold under normal conditions. Treatment with

ROS generating agents (e.g., CNP) results in a further increase of ROS, which cannot be compensated in cancer cells and thus exceeds a threshold finally leading to cytotoxic effects.[30, 52] In contrast, our previous data suggest, that healthy cells are able to counteract increased ROS levels by adaptation of the endogenous antioxidant systems. This adaptation could explain the prevention of TGFβ-1-induced and ROS-mediated myofibroblast formation after CNP treatment, although no direct antioxidant activity was found in the ROS measurement. On the contrary, rather resulted in a small increase of ROS. Nonetheless, a number of studies showed, that there is no persisting oxidative damage in healthy fibroblasts after treatment with CNP, rather a protection against exogenous prooxidative noxes was observed.[51, 72, 81] Possibly, the antioxidant effects of CNP, which would explain the effect on ROS dependent myofibroblast formation and was shown in several studies including our own, is mediated by an induction of the cellular antioxidant system according to the principle of hormesis.[82, 83] In a study of Culcasi et al., it was shown that micromolar concentrations of CNP induce ROS formation at non-toxic levels via NADPH-oxidase activation,[84] which is known to trigger myofibroblast formation.[17] Possibly, after a slight ROS increase, which is shown here after CNP treatment, fibroblasts response with the induction of antioxidant enzymes or other antioxidant defense mechanisms, which in consequence results in a later protection against further ROS inducing agents, like in this study TGF-β1 (here after 24 and 48 hours pretreatment with CNP). In this context, another study with human dermal fibroblasts showed, that glutathione or glutathione oxidase levels were not or only slightly affected by CNP-1 and it was hypothesized that CNP directly scavenge superoxide via their SOD-mimetic activity.[51] However, the toxicity of CNP in diverse tumor cell lines may be the result of a prooxidative activity and increased ROS-sensitivity of tumor cells. However, permanently increased ROS levels cause damage in non-cancerous cells as well, but still tumor cells are more sensitive to an exogenously caused increase of ROS levels.[85–88] In that context it has to be mentioned, that CNP-3, which caused the highest increase of ROS levels in both cell types, were the only of the cerium oxide particles tested here, that showed cytotoxic effect in healthy fibroblasts. Possibly a threshold is exceeded here, which in consequence induces cytotoxicity not only in cancerous cells, but also in fibroblasts. These observations may dismiss this composition of particles for a systemic application in therapy.

In summary, the composition of CNP-3, which were found to exhibit cytotoxic effects in HDF with only a slight prevention of myofibroblast formation, seems to be rather not suitable for a medical application in cancer therapy. Also CNP-4 are not well suitable, as they only showed a weak anti-tumor activity in melanoma cells (no detectable IC_{50} until a concentration of 1.5 mM). In contrast, CNP-1 seem to have the most appropriate properties being an anti-cancer tool due to their selective effects on cell viability of tumor cells and healthy cells and their high anti-invasive impact. Similar beneficial effects were obtained with CNP-2. Regarding to the here investigated biological parameters, with toxicity and invasion to be of great importance in context of cancer therapy, a small size (4.5 nm) and a mixed content of $Ce^{3+}/^{4+}$ appear to be an advantage over a larger size and predominantly Ce^{3+} or Ce^{4+} contents.

Many classical chemotherapeutics, like doxorubicin, show damaging effects on healthy cells and tissues, especially after long term exposure.[89]

To exclude adverse effects of CNP on HDF after long term exposure a long term study over 19 weeks was performed, using CNP-2. We focused on those particles as they are very similar to CNP-1 in the cell biological parameters addressed here, but are also commercially available in high amounts. In HDF, no inhibitory effect of these particles on proliferation was found, rather CNP-2 even promoted proliferation by trend. These results indicate that CNP exert no adverse effects in HDF even after long term exposure and promise no or little side effects on healthy cells throughout a therapeutic application of CNP. The growth stimulation may be the result of antioxidant effects of CNP in normal fibroblasts, either mediated by ROS scavenging or by triggering the endogenous antioxidant defense system of healthy cells.[90]

This study together with recent other studies.[29, 54, 70, 91] show a great potential of CNP for an application as anti-cancer tool, but their biological activity is dependent on several physicochemical and biological factors. For the design of CNP as an anti-cancer tools these factors have to be monitored and the biological activity has to be checked, carefully. The underlying mechanisms, which mediate anti-cancer activity or selectivity in redox-activity or toxicity still have to be elucidated. However, the study herein provides some crucial parameters that need to be considered for the development of save nanoparticles for anti-cancer therapy.

REFERENCES

1. V. Atkinson, Medical management of malignant melanoma. *Aust. Prescr.* 38, 74 (**2015**).
2. B. S. Jayashree, S. Nigam, A. Pai, H. K. Patel, N. D. Reddy, N. Kumar, and C. M. Rao, Targets in anticancer research—A review. *Indian J. Exp. Biol.* 53, 489 (**2015**).
3. S. Rajanna, I. Rastogi, L. Wojdyla, H. Furo, A. Kulesza, L. Lin, B. Sheu, M. Frakes, M. Ivanovich, and N. Puri, Current molecularly targeting therapies in NSCLC and melanoma. *Anticancer Agents Med. Chem.* 15, 856 (**2015**).
4. F. Obrist, G. Manic, G. Kroemer, I. Vitale, and L. Galluzzi, Trial watch: Proteasomal inhibitors for anticancer therapy. *Mol. Cell Oncol.* 2, e974463 (**2015**).
5. S. P. Langdon and D. A. Cameron, Pertuzumab for the treatment of metastatic breast cancer. *Expert Rev. Anticancer Ther.* 13, 907 (**2013**).

6. K. T. Flaherty, Sorafenib: Delivering a targeted drug to the right targets. *Expert Rev. Anticancer Ther.* 7, 617 (**2007**).
7. J. M. Brandner and N. K. Haass, Melanoma's connections to the tumour microenvironment. *Pathology* 45, 443 (**2013**).
8. H. Fang and Y. A. Declerck, Targeting the tumor microenvironment: From understanding pathways to effective clinical trials. *Cancer Res.* 73, 4965 (**2013**).
9. B. Cat, D. Stuhlmann, H. Steinbrenner, L. Alili, O. Holtkotter, H. Sies, and P. Brenneisen, Enhancement of tumor invasion depends on transdifferentiation of skin fibroblasts mediated by reactive oxygen species. *J. Cell Sci.* 119, 2727 (**2006**).
10. O. De Wever and M. Mareel, Role of tissue stroma in cancer cell invasion. *J. Pathol.* 200, 429 (**2003**).
11. L. Mei, W. Du, and W. W. Ma, Targeting stromal microenvironment in pancreatic ductal adenocarcinoma: Controversies and promises. *J. Gastrointest Oncol.* 7, 487 (**2016**).
12. A. A. Rucki and L. Zheng, Pancreatic cancer stroma: Understanding biology leads to new therapeutic strategies. *World J. Gastroenterol.* 20, 2237 (**2014**).
13. O. De Wever, P. Demetter, M. Mareel, and M. Bracke, Stromal myofibroblasts are drivers of invasive cancer growth. *Int. J. Cancer* 123, 2229 (**2008**).
14. L. A. Liotta and E. C. Kohn, The microenvironment of the tumour-host interface. *Nature* 411, 375 (**2001**).
15. U. M. Polanska and A. Orimo, Carcinoma-associated fibroblasts: Non-neoplastic tumour-promoting mesenchymal cells. *J. Cell Physiol.* 228, 1651 (**2013**).
16. O. De Wever and M. Mareel, Role of myofibroblasts at the invasion front. *Biol Chem.* 383, 55 (**2002**).
17. L. Alili, M. Sack, K. Puschmann, and P. Brenneisen, Fibroblast-to-myofibroblast switch is mediated by NAD(P)H oxidase generated reactive oxygen species. *Biosci Rep.* (**2013**).
18. A. Desmouliere, C. Guyot, and G. Gabbiani, The stroma reaction myofibroblast: A key player in the control of tumor cell behavior. *Int. J. Dev. Biol.* 48, 509 (**2004**).
19. Y. Chen, J. Peng, M. Han, M. Omar, D. Hu, X. Ke, and N. Lu, A low-molecular-weight heparin-coated doxorubicin-liposome for the prevention of melanoma metastasis. *J. Drug Target* 23, 335 (**2015**).
20. Y. F. Rao, W. Chen, X. G. Liang, Y. Z. Huang, J. Miao, L. Liu, Y. Lou, X. G. Zhang, B. Wang, R. K. Tang, Z. Chen, and X. Y. Lu, Epirubicin-loaded superparamagnetic iron-oxide nanoparticles for transdermal delivery: Cancer therapy by circumventing the skin barrier. *Small* 11, 239 (**2015**).
21. D. W. Edwardson, R. Narendrula, S. Chewchuk, K. Mispel-Beyer, J. P. Mapletoft, and A. M. Parissenti, Role of drug metabolism in the cytotoxicity and clinical efficacy of anthracyclines. *Curr. Drug Metab.* 16, 412 (**2015**).
22. C. Du, D. Deng, L. Shan, S. Wan, J. Cao, J. Tian, S. Achilefu, and Y. Gu, A pH-sensitive doxorubicin prodrug based on folate-conjugated BSA for tumor-targeted drug delivery. *Biomaterials.* 34, 3087 (**2013**).
23. W. A. Woodward, E. A. Strom, M. D. McNeese, G. H. Perkins, E. L. Outlaw, G. N. Hortobagyi, A. U. Buzdar, and T. A. Buchholz, Cardiovascular death and second non-breast cancer malignancy after postmastectomy radiation and doxorubicin-based chemotherapy. *Int. J. Radiat. Oncol. Biol. Phys.* 57, 327 (**2003**).
24. Y. Yan and A. Grothey, Molecular profiling in the treatment of colorectal cancer: Focus on regorafenib. *Onco Targets Ther.* 8, 2949 (**2015**).
25. R. A. Freitas Jr., What is nanomedicine?. *Dis Mon.* 51, 325 (**2005**).
26. S. V. N. T. Kuchibhatla, A. S. Karakoti, D. Bera, and S. Seal, One dimensional nanostructured materials. *Progress in Materials Science* 52, 699 (**2007**).
27. Q. Qu, X. Ma, and Y. Zhao, Targeted delivery of doxorubicin to mitochondria using mesoporous silica nanoparticle nanocarriers. *Nanoscale* 7, 16677 (**2015**).
28. Y. F. Xiao, J. M. Li, S. M. Wang, X. Yong, B. Tang, M. M. Jie, H. Dong, X. C. Yang, and S. M. Yang, Cerium oxide nanoparticles inhibit the migration and proliferation of gastric cancer by increasing DHX15 expression. *Int. J. Nanomedicine.* 11, 3023 (**2016**).
29. M. Pesic, A. Podolski-Renic, S. Stojkovic, B. Matovic, D. Zmejkoski, V. Kojic, G. Bogdanovic, A. Pavicevic, M. Mojovic, A. Savic, I. Milenkovic, A. Kalauzi, and K. Radotic, Anti-cancer effects of cerium oxide nanoparticles and its intracellular redox activity. *Chem. Biol. Interact.* 232, 85 (**2015**).
30. L. Alili, M. Sack, C. von Montfort, S. Giri, S. Das, K. S. Carroll, K. Zanger, S. Seal, and P. Brenneisen, Downregulation of tumor growth and invasion by redox-active nanoparticles. *Antioxid Redox Signal.* 19, 765 (**2013**).
31. L. Hasandoost, A. Akbarzadeh, H. Attar, and A. Heydarinasab, *In vitro* effect of imatinib mesylate loaded on polybutylcyanoacrylate nanoparticles on leukemia cell line K562. *Artif Cells Nanomed. Biotechnol.* 45, 665 (**2017**).
32. R. Zhang, S. Su, K. Hu, L. Shao, X. Deng, W. Sheng, and Y. Wu, Smart micelle@polydopamine core–shell nanoparticles for highly effective chemo-photothermal combination therapy. *Nanoscale* 7, 19722 (**2015**).
33. M. Sack, L. Alili, E. Karaman, S. Das, A. Gupta, S. Seal, and P. Brenneisen, Combination of conventional chemotherapeutics with redox-active cerium oxide nanoparticles—A novel aspect in cancer therapy. *Mol. Cancer Ther.* 13, 1740 (**2014**).
34. P. Moller, N. R. Jacobsen, J. K. Folkmann, P. H. Danielsen, L. Mikkelsen, J. G. Hemmingsen, L. K. Vesterdal, L. Forchhammer, H. Wallin, and S. Loft, Role of oxidative damage in toxicity of particulates. *Free Radic. Res.* 44, 1 (**2010**).
35. K. Kettler, P. Krystek, C. Giannakou, A. J. Hendriks, and W. H. de Jong, Exploring the effect of silver nanoparticle size and medium composition on uptake into pulmonary epithelial 16HBE14o-cells. *J. Nanopart. Res.* 18, 182 (**2016**).
36. D. Nath Roy, R. Goswami, and A. Pal, Nanomaterial and toxicity: What can proteomics tell us about the nanotoxicology?. *Xenobiotica.* 47, 632 (**2017**).
37. Z. Chen, Y. Wang, L. Zhuo, S. Chen, L. Zhao, X. Luan, H. Wang, and G. Jia, Effect of titanium dioxide nanoparticles on the cardiovascular system after oral administration. *Toxicol Lett.* 239, 123 (**2015**).
38. W. H. De Jong, L. T. Van Der Ven, A. Sleijffers, M. V. Park, E. H. Jansen, H. Van Loveren, and R. J. Vandebriel, Systemic and immunotoxicity of silver nanoparticles in an intravenous 28 days repeated dose toxicity study in rats. *Biomaterials* 34, 8333 (**2013**).
39. G. Oberdorster, E. Oberdorster, and J. Oberdorster, Nanotoxicology: An emerging discipline evolving from studies of ultrafine particles. *Environ Health Perspect.* 113, 823 (**2005**).
40. A. S. Karakoti, N. A. Monteiro-Riviere, R. Aggarwal, J. P. Davis, R. J. Narayan, W. T. Self, J. McGinnis, and S. Seal, Nanoceria as antioxidant: Synthesis and biomedical applications. *JOM (1989)* 60, 33 (**2008**).
41. E. G. Heckert, A. S. Karakoti, S. Seal, and W. T. Self, The role of cerium redox state in the SOD mimetic activity of nanoceria. *Biomaterials.* 29, 2705 (**2008**).
42. C. Walkey, S. Das, S. Seal, J. Erlichman, K. Heckman, L. Ghibelli, E. Traversa, J. F. McGinnis, and W. T. Self, Catalytic properties and biomedical applications of cerium oxide nanoparticles. *Environ. Sci. Nano.* 2, 33 (**2015**).
43. A. Arya, N. K. Sethy, M. Das, S. K. Singh, A. Das, S. K. Ujjain, R. K. Sharma, M. Sharma, and K. Bhargava, Cerium oxide nanoparticles prevent apoptosis in primary cortical culture by stabilizing mitochondrial membrane potential. *Free Radic. Res.* 48, 784 (**2014**).
44. J. M. Dowding, S. Seal, and W. T. Self, Cerium oxide nanoparticles accelerate the decay of peroxynitrite (ONOO(-)). *Drug Deliv. Transl. Res.* 3, 375 (**2013**).
45. S. Chen, Y. Hou, G. Cheng, C. Zhang, S. Wang, and J. Zhang, Cerium oxide nanoparticles protect endothelial cells from apoptosis induced by oxidative stress. *Biol. Trace Elem. Res.* 154, 156 (**2013**).

46. Y. Xue, Q. F. Luan, D. Yang, X. Yao, and K. B. Zhou, Direct evidence for hydroxyl radical scavenging activity of cerium oxide nanoparticles. *Journal of Physical Chemistry C* 115, 4433 **(2011)**.

47. T. Pirmohamed, J. M. Dowding, S. Singh, B. Wasserman, E. Heckert, A. S. Karakoti, J. E. King, S. Seal, and W. T. Self, Nanoceria exhibit redox state-dependent catalase mimetic activity. *Chem. Commun. (Camb).* 46, 2736 **(2010)**.

48. A. S. Karakoti, S. Singh, A. Kumar, M. Malinska, S. V. Kuchibhatla, K. Wozniak, W. T. Self, and S. Seal, PEGylated nanoceria as radical scavenger with tunable redox chemistry. *J. Am. Chem. Soc.* 131, 14144 **(2009)**.

49. L. P. Franchi, B. B. Manshian, T. A. de Souza, S. J. Soenen, E. Y. Matsubara, J. M. Rosolen, and C. S. Takahashi, Cyto- and genotoxic effects of metallic nanoparticles in untransformed human fibroblast. *Toxicol In vitro* 29, 1319 **(2015)**.

50. W. Lin, Y. W. Huang, X. D. Zhou, and Y. Ma, Toxicity of cerium oxide nanoparticles in human lung cancer cells. *Int. J. Toxicol.* 25, 451 **(2006)**.

51. C. von Montfort, L. Alili, S. Teuber-Hanselmann, and P. Brenneisen, Redox-active cerium oxide nanoparticles protect human dermal fibroblasts from PQ-induced damage. *Redox Biol.* 4, 1 **(2015)**.

52. L. Alili, M. Sack, A. S. Karakoti, S. Teuber, K. Puschmann, S. M. Hirst, C. M. Reilly, K. Zanger, W. Stahl, S. Das, S. Seal, and P. Brenneisen, Combined cytotoxic and anti-invasive properties of redox-active nanoparticles in tumor-stroma interactions. *Biomaterials.* 32, 2918 **(2011)**.

53. S. Das, J. M. Dowding, K. E. Klump, J. F. McGinnis, W. Self, and S. Seal, Cerium oxide nanoparticles: Applications and prospects in nanomedicine. *Nanomedicine (Lond).* 8, 1483 **(2013)**.

54. I. Celardo, J. Z. Pedersen, E. Traversa, and L. Ghibelli, Pharmacological potential of cerium oxide nanoparticles. *Nanoscale* 3, 1411 **(2011)**.

55. A. Asati, S. Santra, C. Kaittanis, and J. M. Perez, Surface-charge-dependent cell localization and cytotoxicity of cerium oxide nanoparticles. *ACS Nano.* 4, 5321 **(2010)**.

56. M. K. Xu, Z. H. Ouyang, and Z. R. Shen, Topological evolution of cerium(III) molybdate microflake assemblies induced by amino acids. *Chinese Chemical Letters* 27, 673 **(2016)**.

57. D. J. Giard, S. A. Aaronson, G. J. Todaro, P. Arnstein, J. H. Kersey, H. Dosik, and W. P. Parks, *In vitro* cultivation of human tumors: Establishment of cell lines derived from a series of solid tumors. *J. Natl. Cancer Inst.* 51, 1417 **(1973)**.

58. K. Bayreuther, P. I. Francz, J. Gogol, and K. Kontermann, Terminal differentiation, aging, apoptosis, and spontaneous transformation in fibroblast stem cell systems *in vivo* and *in vitro*. *Ann. N. Y. Acad. Sci.* 663, 167 **(1992)**.

59. A. S. Karakoti, S. V. N. T. Kuchibhatla, K. S. Babu, and S. Seal, Direct synthesis of nanoceria in aqueous polyhydroxyl solutions. *Journal of Physical Chemistry C* 111, 17232 **(2007)**.

60. T. Mosmann, Rapid colorimetric assay for cellular growth and survival: Application to proliferation and cytotoxicity assays. *J. Immunol. Methods* 65, 55 **(1983)**.

61. U. K. Laemmli, Cleavage of structural proteins during the assembly of the head of bacteriophage T4. *Nature* 227, 680 **(1970)**.

62. T. Zheng, S. Bott, and Q. Huo, Techniques for accurate sizing of gold nanoparticles using dynamic light scattering with particular application to chemical and biological sensing based on aggregate formation. *ACS Appl. Mater. Interfaces* 8, 21585 **(2016)**.

63. G. Pulido-Reyes, I. Rodea-Palomares, S. Das, T. S. Sakthivel, F. Leganes, R. Rosal, S. Seal, and F. Fernandez-Pinas, Untangling the biological effects of cerium oxide nanoparticles: The role of surface valence states. *Sci. Rep.* 5, 15613 **(2015)**.

64. J. M. Perez, A. Asati, S. Nath, and C. Kaittanis, Synthesis of biocompatible dextran-coated nanoceria with pH-dependent antioxidant properties. *Small* 4, 552 **(2008)**.

65. Z. A. Qiao, Z. Wu, and S. Dai, Shape-controlled ceria-based nanostructures for catalysis applications. *ChemSusChem.* 6, 1821 **(2013)**.

66. E. G. Heckert, S. Seal, and W. T. Self, Fenton-like reaction catalyzed by the rare earth inner transition metal cerium. *Environ. Sci. Technol.* 42, 5014 **(2008)**.

67. C. J. Szymanski, P. Munusamy, C. Mihai, Y. Xie, D. Hu, M. K. Gilles, T. Tyliszczak, S. Thevuthasan, D. R. Baer, and G. Orr. *Biomaterials.* 62, 147 **(2015)**.

68. L. De Marzi, A. Monaco, J. De Lapuente, D. Ramos, M. Borras, M. Di Gioacchino, S. Santucci, and A. Poma, Cytotoxicity and genotoxicity of ceria nanoparticles on different cell lines *in vitro*. *Int. J. Mol. Sci.* 14, 3065 **(2013)**.

69. E. J. Park, J. Choi, Y. K. Park, and K. Park, Oxidative stress induced by cerium oxide nanoparticles in cultured BEAS-2B cells. *Toxicology* 245, 90 **(2008)**.

70. Y. Gao, K. Chen, J. L. Ma, and F. Gao, Cerium oxide nanoparticles in cancer. *Onco Targets Ther.* 7, 835 **(2014)**.

71. D. Ali, S. Alarifi, S. Alkahtani, A. A. AlKahtane, and A. Almalik, Cerium oxide nanoparticles induce oxidative stress and genotoxicity in human skin melanoma cells. *Cell Biochem. Biophys.* 71, 1643 **(2015)**.

72. J. Colon, L. Herrera, J. Smith, S. Patil, C. Komanski, P. Kupelian, S. Seal, D. W. Jenkins, and C. H. Baker, Protection from radiation-induced pneumonitis using cerium oxide nanoparticles. *Nanomedicine* 5, 225 **(2009)**.

73. S. M. Hirst, A. Karakoti, S. Singh, W. Self, R. Tyler, S. Seal, and C. M. Reilly, Bio-distribution and *in vivo* antioxidant effects of cerium oxide nanoparticles in mice. *Environ. Toxicol.* 28, 107 **(2013)**.

74. S. V. Kuchibhatla, A. S. Karakoti, D. R. Baer, S. Samudrala, M. H. Engelhard, J. E. Amonette, S. Thevuthasan, and S. Seal, Influence of aging and environment on nanoparticle chemistry—Implication to confinement effects in nanoceria. *J. Phys. Chem. C Nanomater. Interfaces* 116, 14108 **(2012)**.

75. Y. Cheng, Y. Li, R. Li, J. Lu, and K. Wang, Orally administrated cerium chloride induces the conformational changes of rat hemoglobin, the hydrolysis of 2,3-DPG and the oxidation of heme-Fe(II), leading to changes of oxygen affinity. *Chem. Biol. Interact.* 125, 191 **(2000)**.

76. Q. Liu, Y. Ding, Y. Yang, L. Zhang, L. Sun, P. Chen, and C. Gao, Enhanced peroxidase-like activity of porphyrin functionalized ceria nanorods for sensitive and selective colorimetric detection of glucose. *Mater. Sci. Eng. C Mater. Biol. Appl.* 59, 445 **(2016)**.

77. X. Liu, N. Huang, H. Li, Q. Jin, and J. Ji, Surface and size effects on cell interaction of gold nanoparticles with both phagocytic and nonphagocytic cells. *Langmuir.* 29, 9138 **(2013)**.

78. J. A. Vassie, J. M. Whitelock, and M. S. Lord, Endocytosis of cerium oxide nanoparticles and modulation of reactive oxygen species in human ovarian and colon cancer cells. *Acta Biomater.* **(2016)**.

79. X. Cui, Reactive oxygen species: The achilles' heel of cancer cells?. *Antioxid Redox Signal* 16, 1212 **(2012)**.

80. P. T. Schumacker, Reactive oxygen species in cancer cells: Live by the sword, die by the sword. *Cancer Cell* 10, 175 **(2006)**.

81. A. Vincent, S. Babu, E. Heckert, J. Dowding, S. M. Hirst, T. M. Inerbaev, W. T. Self, C. M. Reilly, A. E. Masunov, T. S. Rahman, and S. Seal, Protonated nanoparticle surface governing ligand tethering and cellular targeting. *ACS Nano* 3, 1203 **(2009)**.

82. P. Ludovico and W. C. Burhans, Reactive oxygen species, ageing and the hormesis police. *FEMS Yeast Res.* 14, 33 **(2014)**.

83. M. Ristow and K. Schmeisser, Mitohormesis: Promoting health and lifespan by increased levels of reactive oxygen species (ROS). *Dose Response* 12, 288 **(2014)**.

84. M. Culcasi, L. Benameur, A. Mercier, C. Lucchesi, H. Rahmouni, A. Asteian, G. Casano, A. Botta, H. Kovacic, and S. Pietri, EPR spin trapping evaluation of ROS production in human fibroblasts exposed to cerium oxide nanoparticles: Evidence for NADPH oxidase and mitochondrial stimulation. *Chem. Biol. Interact.* 199, 161 **(2012)**.

85. L. B. Sullivan and N. S. Chandel, Mitochondrial reactive oxygen species and cancer. *Cancer Metab.* 2, 17 **(2014)**.

86. M. L. Boland, A. H. Chourasia, and K. F. Macleod, Mitochondrial dysfunction in cancer. *Front Oncol.* 3, 292 **(2013)**.

87. C. Gorrini, I. S. Harris, and T. W. Mak, Modulation of oxidative stress as an anticancer strategy. *Nat. Rev. Drug Discov.* 12, 931 **(2013)**.

88. D. Trachootham, Y. Zhou, H. Zhang, Y. Demizu, Z. Chen, H. Pelicano, P. J. Chiao, G. Achanta, R. B. Arlinghaus, J. Liu, and P. Huang, Selective killing of oncogenically transformed cells through a ROS-mediated mechanism by beta-phenylethyl isothiocyanate. *Cancer Cell* 10, 241 **(2006)**.

89. P. Angsutararux, S. Luanpitpong, and S. Issaragrisil, Chemotherapy-induced cardiotoxicity: Overview of the roles of oxidative stress. *Oxid Med. Cell Longev.* 2015, 795602 **(2015)**.

90. A. L. Popov, N. R. Popova, I. I. Selezneva, A. Y. Akkizov, and V. K. Ivanov, Cerium oxide nanoparticles stimulate proliferation of primary mouse embryonic fibroblasts *in vitro*. *Mater. Sci. Eng. C Mater. Biol. Appl.* 68, 406 **(2016)**.

91. F. Caputo, M. De Nicola, and L. Ghibelli, Pharmacological potential of bioactive engineered nanomaterials. *Biochem. Pharmacol.* 92, 112 **(2014)**.